Author Manuscript

Author Manuscript

Author Manuscript

Author Manuscript

HHS Public Access

Author manuscript

AAPS PharmSciTech. Author manuscript; available in PMC 2019 October 29.

Published in final edited form as:

AAPS PharmSciTech. ; 20(5): 167. doi:10.1208/s12249-019-1377-0.

Preformulation and Evaluation of Tofacitinib as a Therapeutic Treatment for Asthma

Usir S. Younis[1,2,6], **Ernest Vallorz**[3], **Kenneth J. Addison**[4], **Julie G. Ledford**[4,5], **Paul B. Myrdal**[1]

[1]Department of Pharmaceutical Sciences, University of Arizona, Tucson, Arizona, USA.

[2]Biosciences Research Laboratories (BSRL) Building, 1230 N. Cherry Avenue, Tucson, Arizona 85719, USA.

[3]Department of Pharmacology and Toxicology, University of Arizona, Tucson, Arizona, USA.

[4]Department of Cellular and Molecular Medicine, University of Arizona, Tucson, Arizona, USA.

[5]Asthma and Airways Disease Research Center, University of Arizona, Tucson, Arizona, USA.

Abstract

Preformulation studies on tofacitinib citrate, a small molecule JAK3 specific inhibitor, have not been previously reported in literature. We therefore conducted several preformulation studies on tofacitinib citrate, and its free base, to better understand factors that affect its solubility, stability, and solid-state characteristics. Further, the results of the preformulation studies helped facilitate the development of a nebulized formulation of tofacitinib citrate for inhalational delivery to house dust mite allergen-challenged, BALB/c mice as a potential treatment for eosinophilic asthma. The preformulation results indicated tofacitinib having a basic p*Ka* of 5.2, with its stability dependent on pH, ionic strength, and temperature. Degradation of tofacitinib follows apparent first-order kinetics. In order to maximize stability of the drug, ionic strength and temperature should be minimized, with an optimal range pH between 2.0 and 5.0. Additionally, our findings demonstrate that tofacitinib citrate can successfully be nebulized at a suitable droplet size for inhalation (1.2 ± 0.2 μm MMAD) through a nose-only chamber. Animals dosed with tofacitinib citrate demonstrated marked reductions in BAL eosinophils and total protein concentrations following HDM challenge. These data suggest that tofacitinib citrate represents the potential to be an effective therapy for eosinophilic asthma.

Keywords

tofacitinib; tofacitinib citrate; inhalational delivery; eosinophilia; asthma

[6]To whom correspondence should be addressed.(usirsyounis@gmail.com).

Publisher's Note Springer Nature remains neutral with regard to jurisdictional claims in published maps and institutional affiliations.

Author Manuscript Author Manuscript Author Manuscript Author Manuscript

INTRODUCTION

Asthma affects millions of people worldwide, with its prevalence increasing 15% in the last decade among children and adults in the USA alone (1). Asthma is characterized as a pulmonary disease that elicits airway hyperresponsiveness (AHR), fibrosis, and increased proinflammatory cytokine production, resulting in obstruction and remodeling of the airways (2). The first-line therapy for maintenance of chronic asthma is the use of inhaled corticosteroids (ICS), which inhibit inflammatory and immune responses by reducing transcription factors that produce inflammatory cytokines and reducing mucus hypersecretion (3,4). Treatment with corticosteroids has proven adequate in most patients suffering from exacerbations, but there remains a population that fails to respond to this medication (5–9). Further, complications with prolonged used of ICS include osteoporosis, cataracts, diabetes, and corticosteroid resistance for patients with severe asthma (2,7). Therefore, there is a need for a new type of drug therapy to address these gaps in the treatment of chronic asthma.

Several of the proinflammatory cytokines that are upregulated during chronic asthma are potentially modulated by the JAK-STAT (Janus kinase-signal transducers and activators of transcription) pathway. These include, but are not limited to, interleukin-4 (IL-4), interleukin-5 (IL-5), and interleukin-13 (IL-13) (10–14). These three cytokines are primarily responsible for the recruitment, proliferation, and activation of eosinophils, a primary immune cell seen in asthmatics following an allergic response (15,16). Eosinophil activation has been implicated in many of the aforementioned symptoms of asthma (17). Further, the severity of the disease may be characterized by the degree of eosinophilia witnessed with some asthmatics, with eosinophilia being defined as the collection of eosinophils in the airway and increased concentration of eosinophils in peripheral blood (18). Therefore, inhibition of JAK proteins may affect the production of these various proinflammatory, immune processes (19,20), resulting in the suppression of eosinophilia (21–23), potentially becoming a novel treatment for eosinophilic asthma. While the use of mepolizumab, reslizumab, and recently approved benralizumab (humanized, monoclonal antibodies specific for the reduction of IL-5 activity (24–26)), as treatments for eosinophilic asthma are helpful, they are only provided as subcutaneous injections and must be taken in conjunction with corticosteroids.

Tofacitinib, or Xeljanz®, is the first small molecule Janus kinase (JAK) inhibitor to be approved for both moderate and severe rheumatoid arthritis and active psoriatic arthritis, and is currently undergoing clinical trials for several other conditions, such as refractory dermatomyositis (27), variants of alopecia (28), and systemic sclerosis (29). While the relevance of tofacitinib has been explored for psoriasis, ulcerative colitis, and Crohn's disease, much less is known about tofacitinib's potential as a treatment for an allergic airway response, such as asthma. Kudlacz *et al.* 2008 illustrated that tofacitinib citrate, when given *via* subcutaneous infusion, provided a significant anti-inflammatory effect in ovalbumin allergy-induced mice (30). However, no work to date has investigated the direct, pulmonary delivery of the compound *via* inhalation.

Author Manuscript Author Manuscript Author Manuscript Author Manuscript

Our study investigates tofacitinib citrate as a potential treatment for eosinophilic asthma *via* inhalational delivery, which would result in an overall lower dose in comparison to systemic delivery. Little data is available regarding preformulation studies performed on tofacitinib and therefore we aimed to gain a better understanding of the physical and chemical properties of tofacitinib to facilitate the development of formulations, regardless of the dosage form. These results were utilized to create a formulation suitable for aerosol delivery to house dust mite (HDM) allergenchallenged BALB/c mice. Our findings demonstrate that tofacitinib citrate can be successfully formulated and nebulized at a suitable droplet size for inhalation. Additionally, in allergen-challenged mice, tofacitinib citrate is capable of reducing eosinophilia and total protein in lavage fluid, which is indicative of reduced vascular permeability. These data suggest that tofacitinib citrate has the potential to be an effective treatment for eosinophilic asthma, at a lower dose and with direct delivery to the lungs, in comparison to currently marketed medications.

MATERIALS AND METHODS

Materials

Reference standards of tofacitinib and tofacitinib citrate were both purchased from Vesino Industrial Co., Ltd. (Tianjin, China). HPLC grade acetonitrile (ACN) and boric acid were obtained from Fisher Chemical (Fair Lawn, NJ, USA). Ethanol was acquired from Decon Labs (King of Prussia, PA, USA). Ammonium acetate, sodium hydroxide, monopotassium phosphate, disodium phosphate, and hydrochloric acid were purchased from Sigma-Aldrich (St. Louis, MO, USA). Citric acid was obtained from VWR International (West Chester, PA, USA). Sodium chloride and propylene glycol (PG) were acquired from Spectrum Chemical MFG Corp. (New Brunswick, NJ, USA). A Millipore (Billerica, MA, USA) Milli-Q Ultrapure Water purification system with a 0.22-μm filter was used for water. House dust mite allergen was purchased from Greer Labs (Lenoir, NC, USA). Protein BCA (bicinchoninic) assay was acquired from Pierce Biotechnology (Rockford, IL). Cell stain protocol for differential cell count was obtained from DADE Diagnostics (Aquada, PR).

Methods

High-Performance Liquid Chromatography

Reverse-phase high-performance liquid chromatography (HPLC) was used to analyze tofacitinib drug concentrations from known standards and experimental formulations. All samples were analyzed with a Waters 2690 separation module coupled with a Waters 996 photodiode array ultraviolet detector (Waters Corp., Milford, MA, USA). An Alltima HP C18 5 μm 2.1 mm × 150 mm column was used for all samples. A gradient separation method was developed to quantify tofacitinib. A sample injection volume of 10 μL, with an initial mobile phase composition of 85:15% (*v*/*v*) water:0.01 M ammonium acetate in acetonitrile at a flow rate of 0.4 mL/min. After 5.0 min, the mobile phase linearly changed over 30 s to 40:60% (*v*/*v*) water:0.01 M ammonium acetate in acetonitrile at a flow rate of 0.4 mL/min. After 11 min, the mobile phase linearly changed over 30 s back to 85:15% (*v*/*v*) water:0.01 M ammonium acetate in acetonitrile at a flow rate of 0.4 mL/min. The total run time for this method was 15 min, with tofacitinib eluting at 7.6 min, detected at 285 nm. The

Author Manuscript Author Manuscript Author Manuscript Author Manuscript

data were collected and analyzed using Water Empower Pro 2 chromatography data software.

Stability Studies

The long-term effect of pH, temperature, and ionic strength on the stability of tofacitinib citrate was determined using an acetate buffer in the pH range of 4–5, a phosphate buffer in the range of 6–8, and a borate buffer at pH 9. Buffers were prepared at a constant concentration of 0.1 M. Buffers were pH-adjusted as needed with NaOH and HCl, and ionic strength was adjusted with NaCl, as needed. Samples were prepared in triplicate, with a target tofacitinib citrate concentration of 150 μg/mL. Degradation was observed up to 104 weeks at 4, 25, 37, 48, and 67°C. The amount of tofacitinib citrate remaining was determined using the HPLC gradient method, under those conditions mentioned above. No pH change was recorded in any of the samples over the course of the study.

pH and Cosolvent Solubility Studies

Solubilization studies were carried out using tofacitinib citrate. The effect of pH or cosolvent on the solubility of tofacitinib was determined using a universal buffer (31). Samples were prepared using an excess of tofacitinib citrate and adjusted for pH as needed using sodium hydroxide and hydrochloric acid. Samples were monitored for equilibration by HPLC. Following equilibration at room temperature, samples were filtered using a 0.22-μm PTFE filter and assayed by HPLC. The effect of pH was evaluated over a range from 2.8 to 8.5 and the effect of cosolvent was evaluated at pH 7 over a range of 2.5% to 10% *v*/*v* of either ethanol of propylene glycol.

Solid-State Characterization

The solid-state characteristics of tofacitinib and tofacitinib citrate were analyzed using differential scanning calorimetry (DSC) and powder X-ray diffraction (PXRD). Thermal analysis was performed with a Q1000 DSC with an autosampler (TA Instruments, New Castle, DE, USA). Samples were weighed into a standard aluminum pan and crimped with an aluminum lid. Samples were heated at 5°C/min up to 200°C for the free base, and 300°C for the citrate. Powder X-ray diffraction patterns of both reference standards were collected at room temperature with a PanAnalytical X'pert diffractometer (PANalytical Inc., Westborough, MA, USA) with copper (Kα) radiation (λ = 1.5406 Å) at 45 kV (40-mA target current). Scans were taken between 2-theta of 5.00 and 80.00° per minute at ambient temperature. Samples were placed on a silica zero background holder and diffraction was measured with an X-celerator detector.

Nose-Only Chamber Preparation

Before any mice were exposed to the 36-port, nose-only chamber (In-Tox Products, Moriarty, NM), an aqueous solution of 3 mg/mL of tofacitinib citrate was formulated (tofacitinib citrate was added to water until a 3 mg/mL concentration was achieved, then adjusted to pH 3 with a couple drops of 0.1 N HCl) and nebulized through the chamber to determine appropriate dose and aerodynamic particle size. A Philips Respironics Sidestream reusable jet nebulizer was used, with the nose-only chamber being held at 12 in. Hg vacuum

Author Manuscript Author Manuscript Author Manuscript Author Manuscript

pressure and 35 psi air pressure at a 5.2-L/min air flow rate. Dose variation was accomplished on the test chamber by varying the amount of time. Filters were fitted on one of the chambers of the apparatus and collected after each “low-dose” run (15 min of nebulization on test chamber) and “high-dose” run (30 min of nebulization) and soaked in a 50:50 acetonitrile:water solvent to determine dose concentration (32). An aliquot was collected and directly filtered (0.2-μm PTFE membrane) into an HPLC vial, and analyzed for tofacitinib concentration using the previously described gradient method. The resulting concentration values are then used to calculate the dose delivered, with the methods described in detail by Alexander *et al.* 2008 (33). The aerosol properties were measured by a Model 3321 Aerodynamic Particle Sizer (APS). The particle counts, mass mean aerodynamic diameter (MMAD), and geometric standard deviation (GSD) were recorded after each low and high dose.

Experimental Mice

BALB/c female mice (36 total), aged 3–4 weeks, were obtained from The Jackson Laboratory (Bar Harbor, ME, USA) and were housed in the University Animal Care facility at the University of Arizona. Each cage contained four mice, with microisolator pans and sterile water and were provided a NIH-31 Modified Mouse Diet (Harlan Teklad, Madison, WI, USA) *ad libitum*. Animal cages were housed in a constant temperature facility with controlled lighting (12-h light/dark cycles). Animals were treated and handled in accordance with the Institutional Animal Care and Use Committee policies and regulations. Mice were randomized into test groups and weighed on a weekly basis for the duration of the study to ensure their health and well-being were intact. The three groups to be exposed to an aerosol atmosphere were acclimated to the tubes of the 36-port, nose-only dosing chamber while aging to 8 weeks of age.

In vivo Protocol

Table I lists the five different groups of mice in the study, and their experimental conditions. Briefly, once the mice were 8 weeks of age, all mice except those in the control group received the first of three exposures to house dust mite (HDM); mice were anesthetized by isoflurane inhalation and given a 45-μL dose of a 2 mg/mL solution of HDM in normal saline *via* oropharyngeal delivery. Then, each day for the following 3 days after HDM challenge, the appropriate groups receiving treatment (either nebulized vehicle, low dose of tofacitinib citrate, or high dose of tofacitinib citrate) were placed in the nose-only chamber. HDM+LD group was exposed to an aerosolized 3 mg/mL tofacitinib citrate formulation for 15 min; the HDM+HD group was exposed to an aerosolized 3 mg/mL tofacitinib citrate formulation for 30 min; and the HDM+V group was exposed to aerosolized deionized water vehicle for 30 min. The mice were then allowed to rest for 3 days, and the challenge and dosing schedule was repeated for two additional weeks. Twenty-four hours after the last treatment (on week 3), the mice were sacrificed *via* carbon dioxide asphyxiation and harvested. A simple schematic of the timeline of this study is illustrated in Fig. 9a.

Bronchoalveolar Lavage Analysis

Bronchoalveolar lavage (BAL) fluid was obtained *via* tracheal cannulation followed by lavage with 1.5 mL of PBS (with 0.1 mM EDTA) at 25°C. Cells obtained from the BALs

Author Manuscript Author Manuscript Author Manuscript Author Manuscript

were resuspended in RBC lysis buffer (150 mM NH_4Cl, 10 mM $KHCO_3$, 0.1 mM EDTA) and incubated on ice for 10 min. Cells were then resuspended in buffer (HBSS −Ca/−Mg, 10 mM EDTA, 5% FCS) and total leukocyte counts were determined using a hemacytometer. For differential monocyte and eosinophil analysis, 200 μL of BAL fluid was applied to a glass slide using a Cytospin 3 (Shandon, Pittsburgh, PA) and cells were stained using Diff-Quick protocol (DADE Diagnostics, Aquada, PR). Monocyte and eosinophil subpopulations were determined by light microscopy using standard morphological criteria on 100 cells.

For the protein bicinchoninic (BCA) assay, a 1:4 ratio of standard/unknown sample to working reagent was added to each microplate well and mixed thoroughly on a plate shaker for 30 s. The plate was incubated at 37°C for 30 min. The plate was left to cool to room temperature; then, the absorbance was measured at 562 nm on a plate reader. The background value was subtracted from the test values for each sample and the test sample values were interpolated from the standard curve.

RESULTS

Solubility

pH Solubility Profile—The effects of pH solubilization on tofacitinib are presented in Fig. 1. Tofacitinib solubilization was evaluated from pH 2.8 to pH 8.5 and equilibrated at room temperature for 7 days. Tofacitinib solubility was shown to increase exponentially with decreasing pH below its pK_a. The pK_a was determined to be 5.2 by best fit by residual sum squares (RSS) of a theoretical base using the Henderson-Hasselbalch equation, with the total amount of drug in solution being the sum of the ionized and unionized form (assuming the unionized concentration remains constant). This value was in good agreement with the predicted value calculated using the ACD/Labs PhysChem software version 7.0. The intrinsic solubility was determined to be 147 μg/mL. Additionally, tofacitinib was evaluated at pH 2.2 and pH 3.5 where its solubility was determined to be 5.2 mg/mL and 1.8 mg/mL respectively.

Cosolvent Solubility—The effect of two commonly used cosolvents, ethanol and propylene glycol, on tofacitinib solubility were evaluated a pH 7.1 ± 0.3 after an equilibration period of 15 days. Figure 2 shows the exponential increase of the solubility of tofacitinib with increasing volume fraction of both cosolvents and presents the solubilization slopes (σ) obtained for each cosolvent. There is good agreement between the solubilization slope of ethanol and the value predicted according to Eq. 1 (34), which gives a predicted slope of 2.9 based on a CLogP of 1.8.

$$\sigma = 1.143 + 0.939 \log K_{ow} \quad (1)$$

Propylene glycol can be seen to have a greater effect of increasing tofacitinib solubility and has a significantly greater slope than would be predicted by Eq. 2 (35).

$$\sigma = 0.174 + 0.714 \log K_{ow} \quad (2)$$

Author Manuscript Author Manuscript Author Manuscript Author Manuscript

Stability

Effect of pH—The stability of tofacitinib citrate was tested under six different pH conditions, ranging from pH 2.0 to 9.0, utilizing various buffer species such as acetate, citrate, phosphate, and borate. Samples were tested under five different temperature conditions (4, 25, 37, 48, and 67°C) at a constant ionic strength of 0.2 M. Representative kinetic rate profiles for the extended stability of tofacitinib at 37°C (pH 4.0–9.0) can be seen in Fig. 3. The kinetic rate profiles in Fig. 3 illustrate tofacitinib citrate degrading under apparent first-order kinetics from pH values 2.0 to 9.0. The pH values below 4.0 (data not shown) parallel the same stability as the samples between pH 4.0–6.0, even at accelerated conditions (67°C). However, tofacitinib citrate degraded more quickly under more basic conditions, with the highest rate of degradation occurring at pH 9.0. These data were further analyzed by Eq. 3 which was used to calculate the degradation rate constants (κ) from the slope of each log-linear best fit regression line. The rate constants were then used to plot a representative pH-rate profile for tofacitinib citrate at 37°C (Fig. 4).

$$\kappa = - \text{ slope } \times 2.303 \tag{3}$$

The natural logarithm of the degradation rate constants for pH values at 5.0 and below could not be calculated due to the samples having a non-negative slope over the course of the study. With a slope value of 2.1, Fig. 4 demonstrates tofacitinib citrate undergoing base-catalyzed degradation, as well as other possible mechanism(s) of degradation that were not explored in this study.

Effect of Ionic Strength—The stability of tofacitinib citrate was tested under four different pH conditions, ranging from pH 2.0 to 9.0, with five different ionic strength buffer solutions ranging from 0.2 to 4.0 M. Samples were tested for 2 weeks at accelerated conditions, 67°C.

The rates of degradation (k) are shown as a function of ionic strength (Fig. 5). The lowest ionic strength (0.2 M) corresponds to the ionic strength used in both the pH and temperature dependent stability studies. The rank order of stability for the different pH values is the same at low ionic strengths, as in Fig. 3, with low pH being more stable. However, as ionic strength is increased, the degradation rate of the pH 9.0 formulation significantly decreases and is equivalent to the pH 2.0 degradation rate in a 4.0-M buffered system.

Effect of Temperature—The Arrhenius equation (Eq. 4) relates the degradation rate constant (calculated for pH stability) to temperature:

$$\kappa = Ae^{-E_a/RT} \tag{4}$$

where κ is the degradation rate constant, A is the frequency of collisions, E_a is the activation energy, R is the gas constant, and T is temperaturein Kelvin. Equation 4 can be expressed in terms of the natural log of the degradation constant, seen below as Eq. 5:

Author Manuscript Author Manuscript Author Manuscript Author Manuscript

$$\ln\kappa = -\left(\frac{E_a}{R}\right)\frac{1}{T} + lnA \quad (5)$$

When Eq. 5 is plotted as *ln κ versus 1/T*, the equation of the linear regression of the best fit line provides the values for activation energy (-slope/R) and the frequency of collisions (y-intercept).These values can then be substituted back into Eq. 5 so that the stability of tofacitinib citrate can be predicted at any temperature, assuming the degradation mechanism remains constant over the given temperature range. Using the degradation data gathered for tofacitinib citrate at 25, 37, 48, and 67°C, an Arrhenius plot is demonstrated in Fig.6. Virtually, no degradation was seen experimentally at 4°C; therefore, the data for these temperatures are not present in the Arrhenius graph.

Solid-State Characteristics—An overlay of the DSC thermograms of tofacitinib and tofacitinib citrate is illustrated in Fig. 7. The thermogram for the free base of tofacitinib shows two endotherms (downward peaks): the first with a peak maximum value at 157.9°C and the second endotherm at 173.4°C. In contrast, the DSC thermogram of tofacitinib citrate has one distinct endotherm that occurred at 212.6°C. This endotherm was deemed to be the melting point of tofacitinib citrate. The raw material of both compounds were further analyzed with powder X-ray diffraction (PXRD) to confirm their identities and crystallinity. An overlay of the XRD diffraction patterns are shown in Fig. 8.

Differential Cell Counts—Figure 9b and c illustrate the results of the differential cell counts of monocytes and eosinophils from BAL fluid, respectively. The number of monocytes was highest in the control group and were decreased for the other four experimental groups. No significant difference in monocytes were seen between the HDM only and the HDM+V group. However, both the low-dose and high-dose groups had a statistically significant increase in monocytes in comparison to the HDM only and HDM+V mice.

In contrast, no eosinophils were seen in the vehicle control group. Eosinophils were present in the other four experimental groups that received HDM. Similar to the monocyte results, no significant difference was seen between the HDM only and HDM+V groups for percentage of eosinophils present. However, both the low-dose and the high-dose mice illustrated statistically significant decreases in eosinophils in comparison to the HDM only and HDM+V mice.

Protein BCA Assay—The total protein concentration gathered from the BAL fluid from all experimental groups is illustrated in Fig. 9d. A statistically significant increase in protein concentration was seen between the control and HDM+V mice. However, total protein concentration was significantly decreased in both the HDM+LD- and HDM+HD-treated mice when compared to the HDM+V group. The drug treatment groups were not statistically significant from the control group.

Filter Content for Dose Variability and Particle Size—It was determined that dose variation was indeed accomplished by varying the amount of time the mice spent on the

Author Manuscript Author Manuscript Author Manuscript Author Manuscript

apparatus. For animals in the low-dose group, an average dose of 1.1 ± 0.03 mg/kg was administered, while the high-dose group received an average dose of 2.3 ± 0.03 mg/kg (dosing levels set based on studies performed by Kudlacz *et al.* 2008). These values represent the inhaled dose; however, they do not reflect the actual amount of drug within each animal. The average aerodynamic particle size for both groups was 1.2 ± 0.2 μm (mass median aerodynamic diameter) with a GSD of 1.79. These results provided confidence that the nose-only chamber was adequately prepared for mice exposure to drug treatment.

DISCUSSION

The JAK3 inhibitor, tofacitinib citrate, currently on the market for rheumatoid and psoriatic arthritis, shows great potential for the treatment of eosinophilic asthma. However, little data is available regarding any preformulation studies performed on tofacitinib. Our research gains a better understanding of tofacitinib's physical and chemical properties to optimize the development of various types of formulations, regardless of the delivery format. Further, the data gathered from the completed preformulation studies were used to successfully develop a feasible nebulized formulation of tofacitinib citrate, delivered to HDM immune-compromised, BALB/c mice. Inhalational delivery of a JAK inhibitor for the treatment of allergic responses due to asthma has not been previously investigated.

In order to achieve the ideal particle size for deep lung penetration while using an Aero-Tech II nebulizer through the 36port nose-only chamber, the solubility of tofacitinib must be between 2.5 and 5 mg/mL. This concentration is based on previous inhalation studies performed by Karlage *et al.* 2010 (32) and Myrdal *et al.* 2007 (36), who determined that the 2.5–5 mg/mL concentration range produced appropriately sized particles (between 1.5–2 μm) and particle count out of the chamber for adequate lung penetration and exposure. With tofacitinib's aqueoussolubilityrangingfrom1.8to5.2 mg/mLbetweenpHvalues3.5 and 2.2, respectively (Fig. 1), an aqueous solution below pH 3.5 would be needed in order to achieve the optimal concentration range for nebulized drug delivery of tofacitinib.

Further, tofacitinib citrate with a 10% volume fraction of ethanol or propylene glycol had a significant increase in solubility, 0.251 mg/mL and 0.341 mg/mL, respectively (Fig. 2), in comparison to its intrinsic solubility of 0.147 mg/mL. However, this increase is not sufficient for the 2.5 mg/mL drug load required for *in vivo* testing. While increasing ethanol or propylene glycol levels beyond 10% would eventually provide solubility greater than 2.5 mg/mL, significant inhalation of cosolvents risks lung irritation (37). As such, other means of solubilization strategies are required for inhalational drug delivery; however, this data may be useful for other modes of drug delivery.

The kinetic rate profiles in Fig. 3 illustrate tofacitinib citrate degrading under apparent first-order kinetics. Tofacitinib citrate degraded more quickly under more basic conditions, with the highest rate of degradation occurring at pH 9.0. This was an ideal outcome, given that tofacitinib must be formulated under acidic conditions (below pH 3.5) in order to have the optimal concentration for nebulized drug delivery (as provided by the aqueous solubility data). Tofacitinib was so stable that the natural logarithm of the degradation rate constants for pH 2.0 through pH 5.0 could not be calculated due to the samples essentially having zero

Author Manuscript Author Manuscript Author Manuscript Author Manuscript

degradation over the course of the study (Fig. 4). This same trend was observed when evaluating the effect ionic strength had on the degradation of tofacitinib citrate (Fig. 5). However, as the concentration of ionic strength increased to a 4.0-M buffered system, the formulations made under basic conditions (pH 9.0) had stability equivalent to the acidic formulations. While formulating under basic conditions are not optimal for inhalational delivery due to tofacitinib's low intrinsic solubility, this data could be useful to stabilize tofacitinib for other routes of drug delivery. Further, the degradation of tofacitinib citrate increases as temperature increases (Fig. 6), with virtually no degradation observed for any of the samples prepared between pH 2.0 and 9.0 at 4°C, over the course of the study. These data allowed us to create a stable, nebulized formulation under acidic conditions (pH 3.0), stored at 4°C that would not degrade during the duration of *in vivo* treatment. It should be noted that despite the lung's large buffering capacity, nebulized solutions below pH 3.0 or above 7.4 may cause adverse effects and further the irritation caused from lung inflammatory diseases. However, those considerations were beyond the scope of this study.

Analysis of tofacitinib and tofacitinib citrate *via* DSC displays endothermic events in both thermograms, indicating a melt and therefore suggesting the material was crystalline (Fig. 7). Tofacitinib citrate and its free base were confirmed to be crystalline solids after analysis utilizing powder X-ray diffraction (Fig. 8). Therefore, both drugs remained intact and did not decompose prior to melting.

After the mice were challenged following an HDM challenge and treatment model (Fig. 9a), bronchoalveolar lavage fluid was harvested and differential cell counts were analyzed. As expected, the majority (> 95%) of cells detected in the BAL of the healthy, unchallenged lungs were macrophages. As lungs are challenged with HDM to induce allergic airways disease, the amount of monocytes should theoretically decrease, while eosinophils, which would be newly migrated to the injured tissue, would increase. The migration of eosinophils to the asthmatic lungs would create a positive feedback system, resulting in the production of more inflammatory cytokines that would initiate a signal for further migration of more eosinophils. Therefore, it was expected that the administration of tofacitinib citrate would not only increase the percentage of monocytes in the total leukocyte cell count collected from BAL fluid of both treatment groups as compared to vehicle, but that the percentage of eosinophils would subsequently decrease with tofacitinib citrate treatment. Figure 9b and c validate these hypotheses. Virtually, no eosinophils were seen in the control group, which had a high monocyte percentage, which would be as expected since the control mice were not exposed to any allergen challenge or drug treatment. The HDM group had a drastic decrease in monocytes in comparison to the control group, and a significant increase in eosinophils from control. The HDM+V group also had a low percentage of monocytes and a high percentage of eosinophils, but was not statistically significant from the HDM group. This confirms that the drug vehicle had no effect on the immune cell count. However, the low-dose tofacitinib citrate group (HDM+LD) and the high-dose tofacitinib citrate group (HDM+HD) both showed a statistically significant increase in monocyte percentage, while they both illustrated a statistically significant decrease in eosinophil percentage. These findings are promising, highlighting the likelihood of tofacitinib citrate delivered *via* inhalation may provide a measurable and positive impact on HDM allergic airways mouse model of asthma. Further, the HDM+LD and HDM+HD groups did not illustrate a

Author Manuscript Author Manuscript Author Manuscript Author Manuscript

statistically significant increase from one another, implying that even though the HDM+HD group was double the dose of the low-dose group, it might not have been high enough to demonstrate a varied dose response.

Further analysis of BAL fluid was done with a protein BCA assay. Healthy, unchallenged lungs would be expected to have a lower protein concentration than HDM-challenged lungs, with the rationale being that lung damage would result in more proteins in the BAL, due to the heightened state of inflammation and vascular permeability. As lungs are damaged, especially in cases of severe inflammation, albumin (one of the most abundant proteins in the bloodstream), finds its way into lung tissue and airspaces due to weakened pulmonary vessels (38). A statistically significant increase in protein concentration was seen between the control and HDM+V mice, which is thought to correlate with a heightened level of tissue damage and/or vascular permeability (Fig. 9d). However, total protein concentration was significantly decreased in both the HDM+LD- and HDM+HD-treated mice when compared to the HDM+V group. The drug treatment groups were not statistically significant from the control group, implying that protein concentrations in the lungs were able to decrease low enough from their damaged state.

CONCLUSIONS

Tofacitinib has been shown to undergo apparent first-order degradation *via* base catalysis in aqueous conditions. The stability of tofacitinib is dependent on pH, ionic strength, and temperature, with maximum stability achieved under acidic conditions (below pH 5.0), at low temperatures and ionic strengths. Solubility of tofacitinib can be manipulated with pH, with its solubility increasing below its pKa of 5.2. Solid-state characterization has determined tofacitinib and its salt form, tofacitinib citrate, to be crystalline solids. When formulated as an aerosol for inhalational delivery to HDM-challenged, BALB/c mice, tofacitinib citrate was able to decrease eosinophils in BAL fluid, as well as decreasing total protein concentration. These studies provide basic preformulation guidelines, not previously reported in literature, to aid in the formulation of tofacitinib regardless of the mode of delivery. Further, this data shows the successful delivery of tofacitinib citrate *via* inhalation, with the possibility of the drug being used to alleviate eosinophilic asthma.

ACKNOWLEDGEMENTS

We would like to thank the American Foundation of Pharmaceutical Education (AFPE) for providing Usir Younis with the Lynn Van Campen Award in Formulation Design, Pre-Doctoral Fellowship for 2 years to help fund this research.

REFERENCES

1. Asthma’s impact on the nation: data from the CDC National Asthma Control Program. Center for Disease Control (CDC) and Prevention, Atlanta. 2012 http://www.cdc.gov/asthma/impacts_nation/asthmafactsheet.pdf. Accessed 13 Feb 2015.
2. Bryan S, Leckie M, Hansel T, Barnes P. Novel therapy for asthma. Expert Opin Investig Drugs. 2000;9:25–42.
3. Bousquet J, Jeffrey P, Busse W, Johnson M, Vignola A. Asthma: from bronchoconstriction to airways inflammation and remodeling. Am J Respir Crit Care Med. 2000;161:1720–45. [PubMed: 10806180]

Author Manuscript Author Manuscript Author Manuscript Author Manuscript

4. Vanacker NJ, Palmans E, Pauwels RA, Kips JC. Effect of combining salmeterol and fluticasone on the progression of airway remodeling. Am J Respir Crit Care Med. 2002;166:1128–34. [PubMed: 12379559]
5. Siddiqui S, Redhu N, Ojo O, Liu B, Irechukwu N, et al. Emerging airway smooth muscle targets to treat asthma. Pulm Pharmacol Ther. 2013;26:132–44. [PubMed: 22981423]
6. Lam J, Levine S. The role of tyrosine kinases in the pathogenesis and treatment of lung disease, advances in protein kinases. In: Biochemistry, genetics and molecular biology. Rijeka, 2012 p. 181–212.
7. Ward C, Pais M, Bish R, Reid D, Feltis B, Johns D, et al. Airway inflammation, basement membrane thickening and bronchial hyperresponsiveness in asthma. Thorax. 2002;57:309–16. [PubMed: 11923548]
8. Vanacker NJ, Palmans E, Pauwels RA, Kips JC. Dose-related effect of inhaled fluticasone on allergen-induced airway changes in rats. Eur Respir J. 2002;20:873–9. [PubMed: 12412678]
9. Vanacker NJ, Palmans E, Kips JC, Pauwels RA. Fluticasone inhibits but does not reverse allergen-induced structural airway changes. Am J Respir Crit Care Med. 2001;163:674–9. [PubMed: 11254522]
10. Kontzias A, Kotlyar A, Laurence A, Changelian P, O'Shea J. Jakinibs: a new class of kinase inhibitors in cancer and autoimmune disease. Curr Opin Pharmacol. 2012;12:464–70. [PubMed: 22819198]
11. Drazen J, Arm J, Austen K. Sorting out the cytokines of asthma. J Exp Med. 1996;183:1–5. [PubMed: 8551212]
12. Kips J. Cytokines in asthma. Eur Respir J. 2001;18:24–33.
13. Chung K, Barnes P. Cytokines in asthma. Thorax. 1999;54:825–57. [PubMed: 10456976]
14. Wong WS. Inhibitors of the tyrosine kinase signaling cascade for asthma. Curr Opin Pharmacol. 2005;5:264–71. [PubMed: 15907913]
15. Licona-Limon P, Kim LK, Palm NW, Flavell RA. TH2, allergy and group 2 innate lymphoid cells. Nat Immunol. 2013;14:536–42. [PubMed: 23685824]
16. Blanchard C, Rothenburg ME. Biology of the eosinophil. Adv Immunol. 2009;101:81–121. [PubMed: 19231593]
17. Rosenberg HF, Dyer KD, Foster PS. Eosinophils: changing perspectives in health and disease. Nat Rev Immunol. 2013;13:9–22. [PubMed: 23154224]
18. Dy ABC, Tanyaratsrisakul S, Voelker DR, Ledford JG. The emerging roles of surfactant protein-A in asthma. J Clin Cell Immunol. 2018;9(4):553–68. [PubMed: 30123671]
19. Malaviya R, Laskin D, Malaviya R. Janus kinase-3 dependent inflammatory responses in allergic asthma. Int Immunopharmacol. 2010;10:829–36. [PubMed: 20430118]
20. Ashino S, Takeda K, Li H, Taylor V, Joetham A, Pine PR, et al. Janus kinase 1/3 signaling pathways are key initiators of Th2 differentiation and lung allergic responses. J Allergy Clin Immunol. 2014;133:1162–74. [PubMed: 24365136]
21. Green RH, Brightling CE, McKenna S, Hargadon B, Parker D, Bradding P, et al. Asthma exacerbations and sputum eosinophil counts: a randomized controlled trial. Lancet. 2002;360:1715–21. [PubMed: 12480423]
22. Parra E, Perez-Gil J. Composition, structure and mechanical properties define performance of pulmonary surfactant membranes and films. Chem Phys Lipids. 2015;185:153–75. [PubMed: 25260665]
23. Wright JR. Immunoregulatory functions of surfactant proteins. Nat Rev Immunol. 2005;5:58–68. [PubMed: 15630429]
24. Abonia JP, Putnam PE. Mepolizumab in eosinophilic disorders. Expert Rev Clin Immunol. 2011;7(4):411–7. [PubMed: 21790283]
25. Pelaia C, Vatrella A, Bruni A, Terracciano R, Pelaia G. Benralizumab in the treatment of severe asthma: design, development and potential place in therapy. Drug Des Dev Ther. 2018;12:619–28.
26. Hom S, Pisano M. Reslizumab (Cinqair): an interleukin-5 antagonist for severe asthma of the eosinophilic phenotype. Pharm Ther. 2017;42(9):564–8.

Author Manuscript Author Manuscript Author Manuscript Author Manuscript

27. Bethesda (MD): U.S. National Library of Medicine; 2018- Study of tofacitinib in refractory dermatomyositis; [about 1p.]. Available from: http://clinicaltrials.gov/. ClinicalTrials.gov Identifier: NCT03002649 Accessed 22 Aug 2018.

28. Bethesda (MD): U.S. National Library of Medicine; 2017-Tofacitinib for the treatment of alopecia areata and its variants; [about 1p.]. Available from: http://clinicaltrials.gov/. ClinicalTrials.gov Identifier: NCT02312882 Accessed 22 Aug 2018.

29. Bethesda (MD): U.S. National Library of Medicine; Evaluation of tofacitinib in early diffuse cutaneous system sclerosis (dcSSc) (TOFA-SSc); [about 1p.]. Available from: http://clinicaltrials.gov/. ClinicalTrials.gov Identifier: NCT03274076 Accessed 22 Aug 2018.

30. Kudlacz E, Conklyn M, Andersen C, Whitney-Pickett C, Changelian P. The JAK-3 inhibitor CP-690550 is a potent anti-inflammatory agent in a murine model of pulmonary eosinophilia. Eur J Pharmacol. 2008;582:154–61. [PubMed: 18242596]

31. Ostling S, Virtama P. A modified preparation of the universal buffer described by Teorell and Stenhagen. Acta Physiol. 1946;11(4):289–93.

32. Karlage KL, Mogalian E, Jensen A, Myrdal PB. Inhalation of an ethanol-based zileuton formulation provides a reduction of pulmonary adenomas in the A/J mouse model. AAPS PharmSciTech. 2010;11:168–73. [PubMed: 20101484]

33. Alexander DJ, Collins CJ, Coombs DW, Gilkison IS, Hardy CJ, Healey G, et al. Association of inhalation toxicologists (AIT) working party recommendation for standard delivered dose calculation and expression in non-clinical aerosol inhalation toxicology studies with pharmaceuticals. Inhal Toxicol. 2008;20:1179–89. [PubMed: 18802802]

34. Machatha SG, Yalkowsky SH. Estimation of the ethanol/water solubility profile from the octanol/water partition coefficient. Int J Pharm. 2004;286(1–2):111–5. [PubMed: 15501007]

35. Yalkowsky SH, Rubino JT. Solubilization by cosolvents I: organic solutes in propylene glycol-water mixtures. J Pharm Sci. 1985;74(4):416–21. [PubMed: 3999002]

36. Myrdal PB, Karlage K, Kuehl PJ, Angersbach BS, Merrill BA, Wightman PD. Effects of novel 5-lipoxygenase inhibitors on the incidence of pulmonary adenomas in the A/J murine model when administered via nose-only inhalation. Carcinogenesis. 2007;28:957–61. [PubMed: 17114645]

37. Montharu J, Le Guellec S, Kittel B, Rabemampianina Y, Guillemain J, et al. Evaluation of lung tolerance of ethanol, propylene glycol, and sorbitan monooleate as solvents in medical aerosols. J Aerosol Med Pulm Drug Deliv. 2010;23(1):41–6. [PubMed: 20131984]

38. Ledford JG, Mukherjee S, Kislan MM, Nugent JL, Hollingsworth JW, et al. Surfactant protein-A suppresses eosinophil-mediated killing of Mycoplasma pneumonia in allergic lungs. Public Libr Sci One. 2012;7:1–12.

Author Manuscript Author Manuscript Author Manuscript Author Manuscript

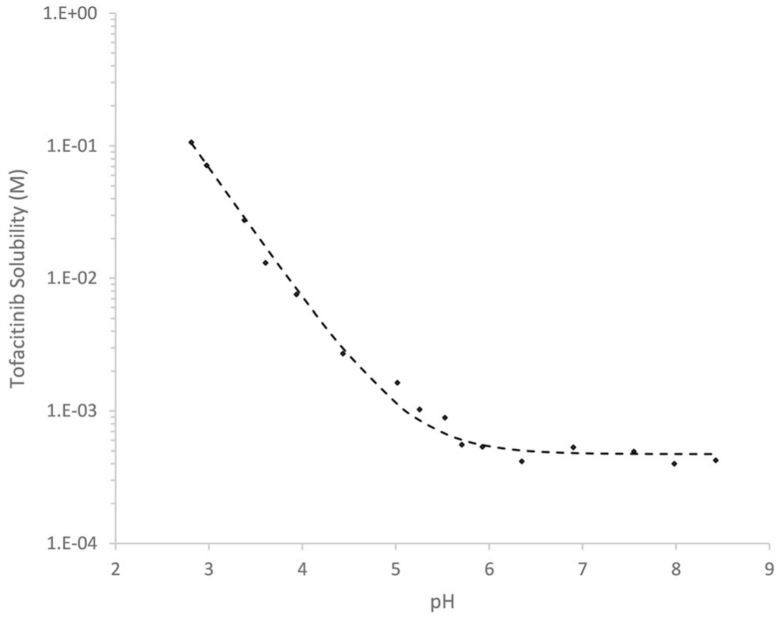

Fig. 1.

The solubilization of tofacitinib as a function of pH. The dotted line represents the predicted solubilities using the Henderson-Hasselbalch equation, with a p*K*a of 5.16

Author Manuscript Author Manuscript Author Manuscript Author Manuscript

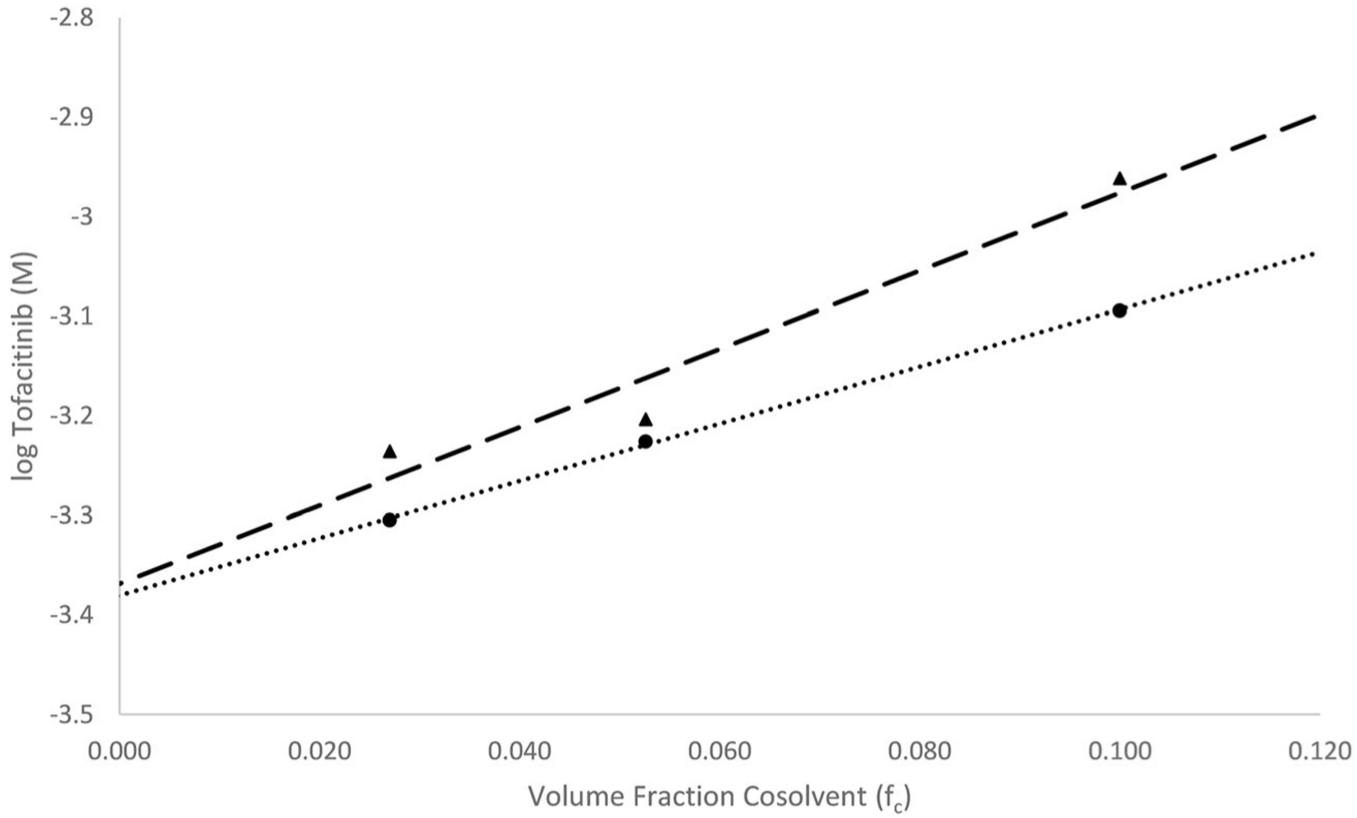

Fig. 2.

The solubilization of tofacitinib by ethanol and propylene glycol. (black circle, ethanol; black up-pointing triangle, propylene glycol)

Author Manuscript Author Manuscript Author Manuscript Author Manuscript

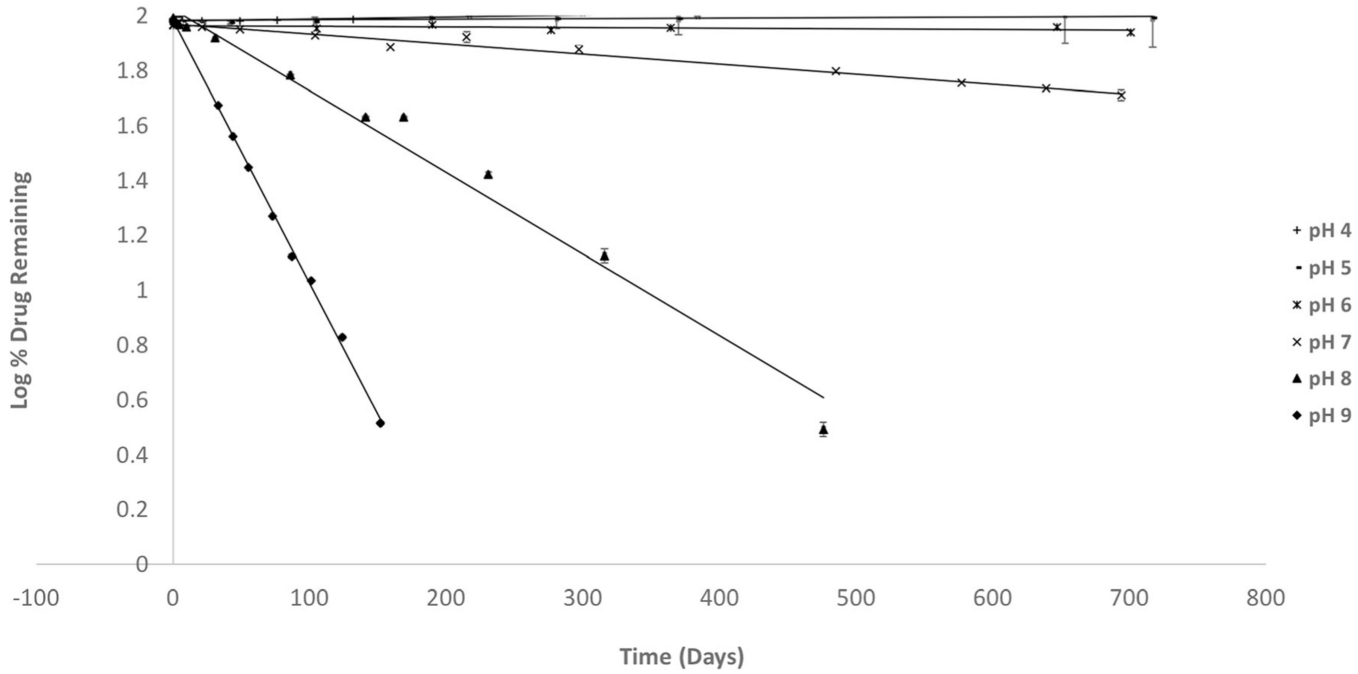

Fig. 3.

Log percent (%) of tofacitinib citrate remaining versus time (days) at pH values between 4.0 and 9.0 at 37°C. (n= 3; SD)

Author Manuscript Author Manuscript Author Manuscript Author Manuscript

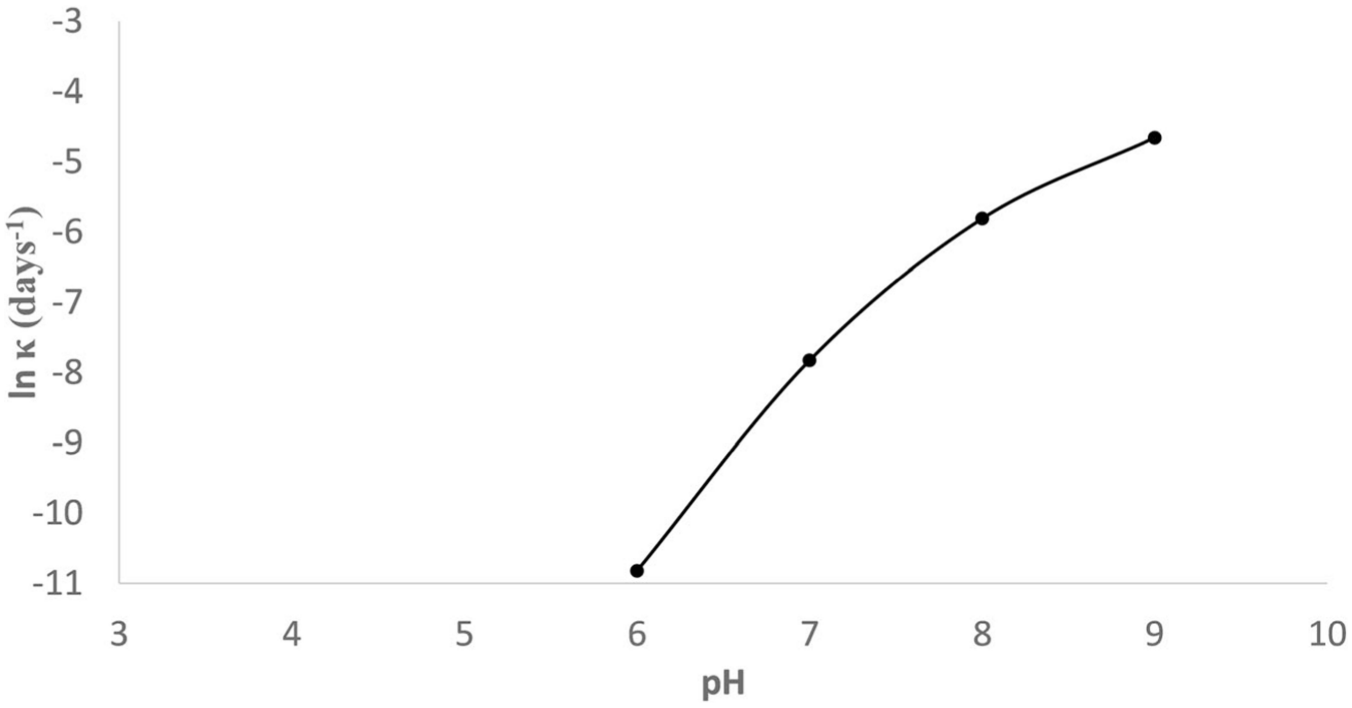

Fig. 4.

Tofacitinib citrate pH-rate profile, with the natural log of the degradation rate constant (κ) plotted against pH, at 37°C

Author Manuscript Author Manuscript Author Manuscript Author Manuscript

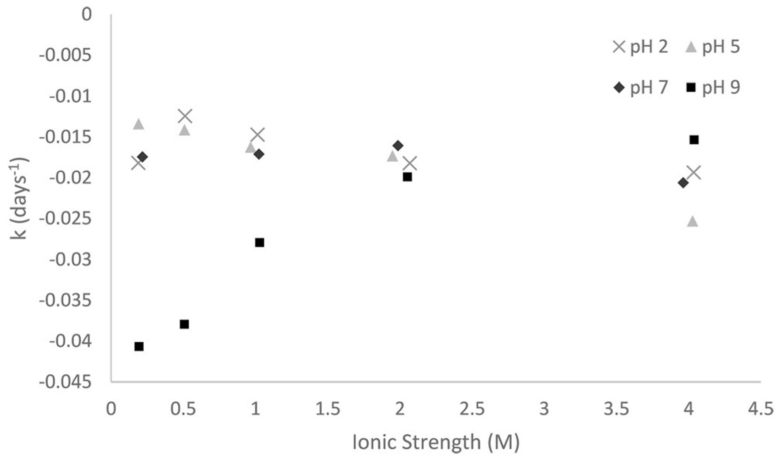

Fig. 5.
Effect of ionic strength on tofacitinib aqueous stability

Author Manuscript Author Manuscript Author Manuscript Author Manuscript

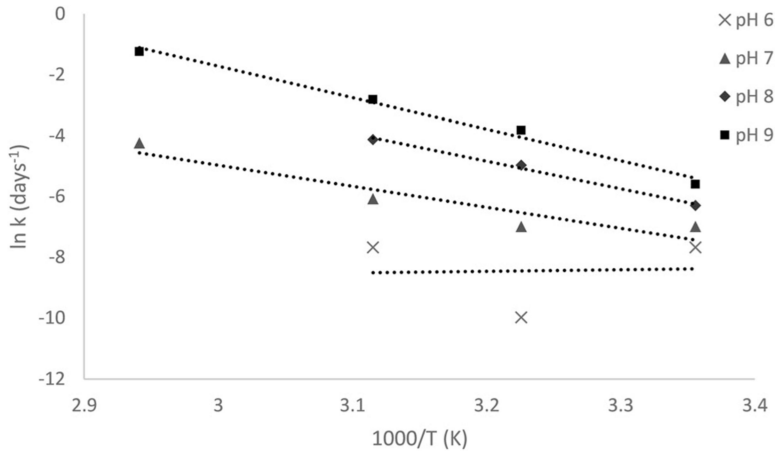

Fig. 6.
Arrhenius plot for tofacitinib citrate

Author Manuscript Author Manuscript Author Manuscript Author Manuscript

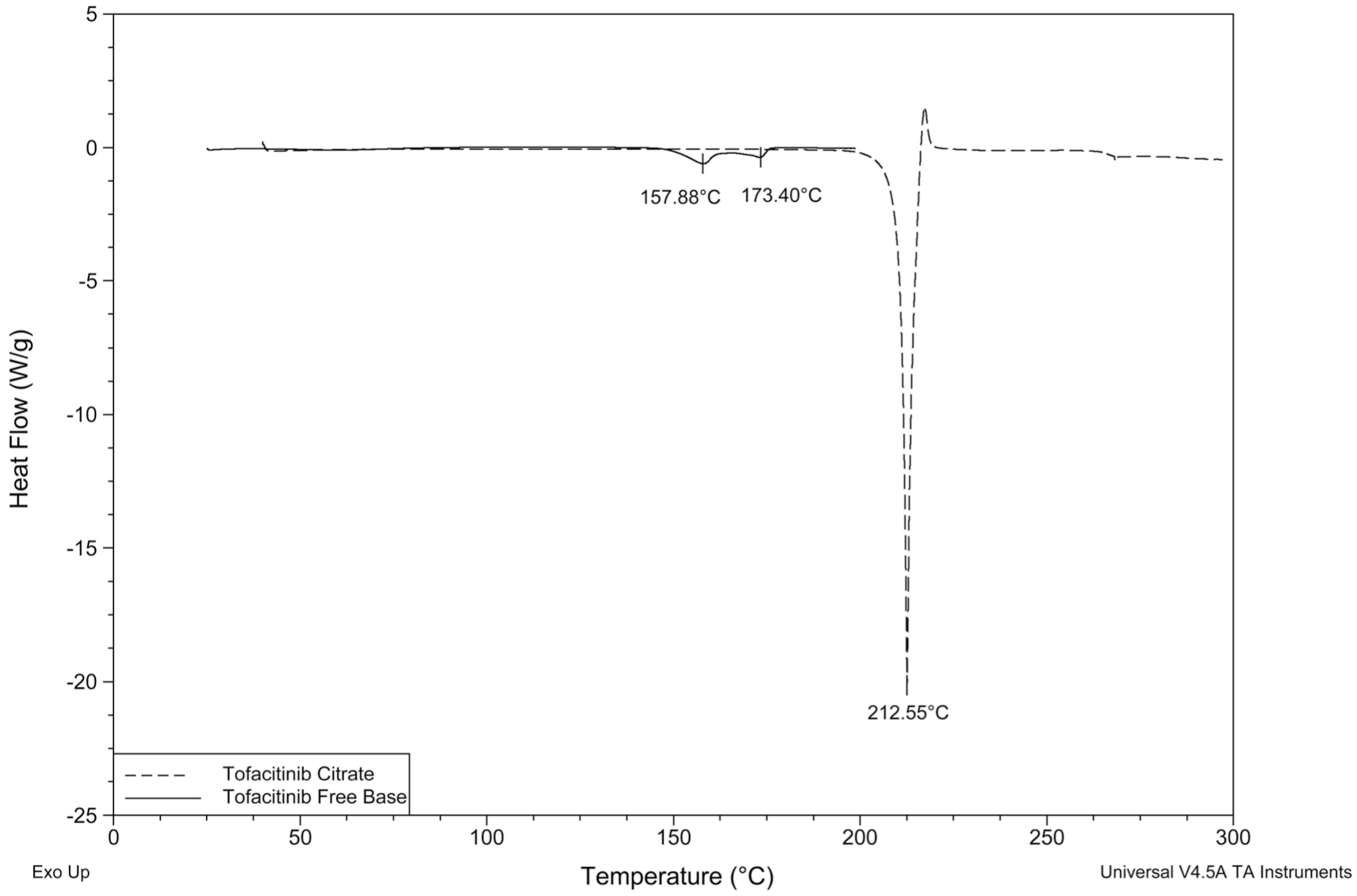

Fig. 7.
DSC thermogram overlay of tofacitinib citrate and tofacitinib free base

Author Manuscript Author Manuscript Author Manuscript Author Manuscript

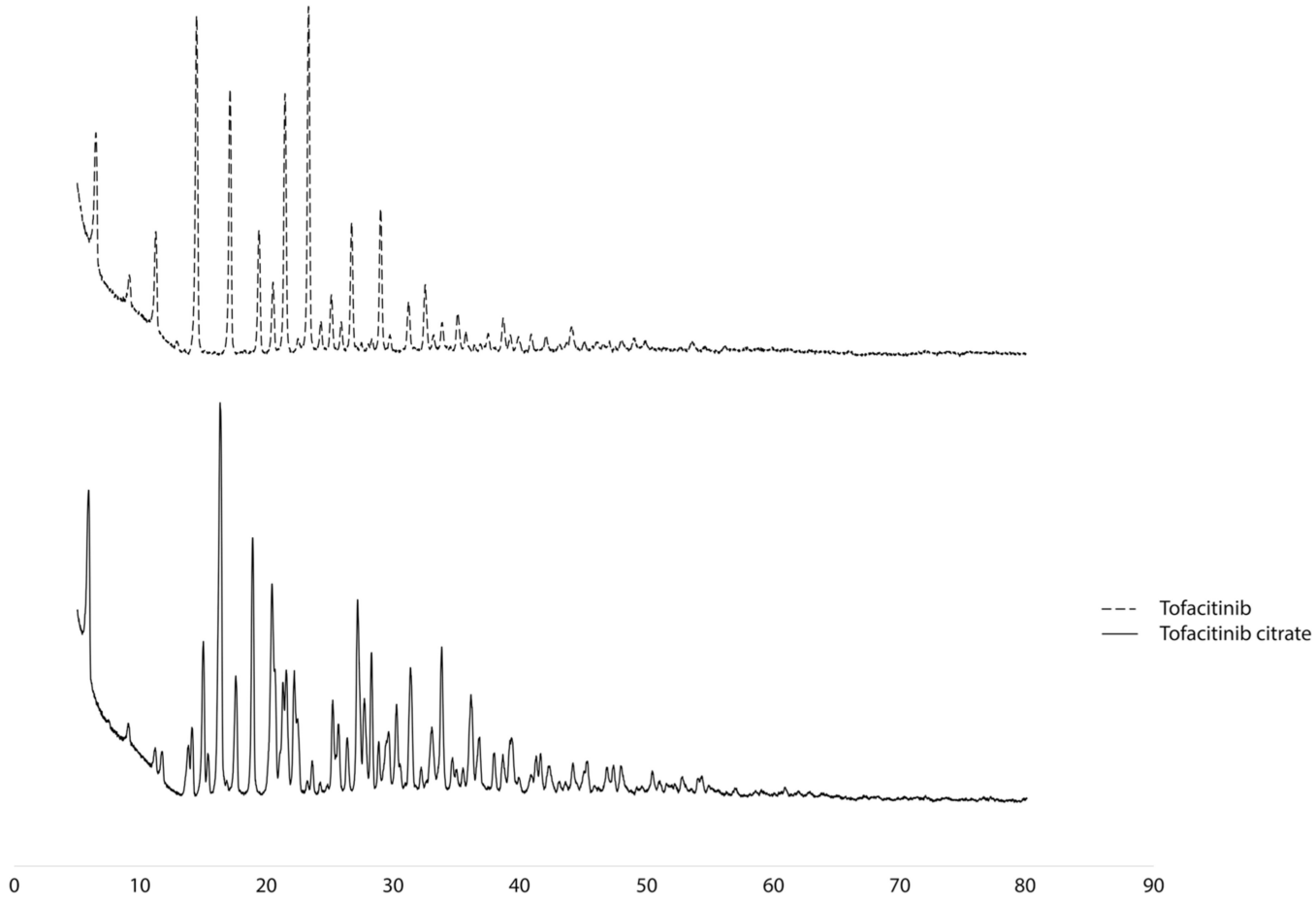

Fig. 8.
An overlay of the crystal diffraction patterns of tofacitinib and tofacitinib citrate

Author Manuscript Author Manuscript Author Manuscript Author Manuscript

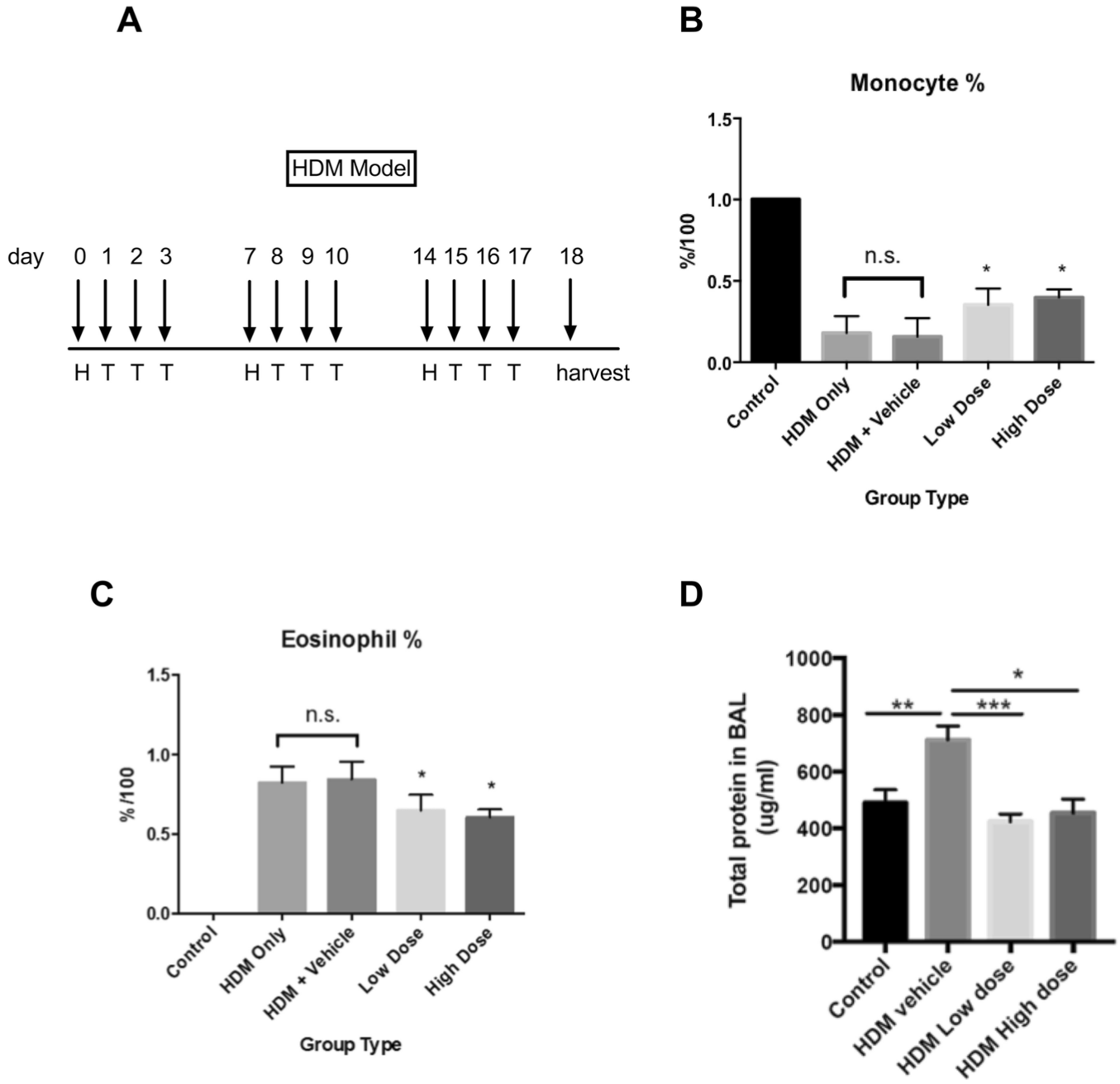

Fig. 9.

a Female, BALB/c mice were challenged in a standard HDM protocol, with HDM delivered intranasally on days 0, 7, and 14 (H). Mice were treated (T) with tofacitinib (or vehicle) *via* inhalation for three consecutive days, 24 h after each HDM challenge (on days 1, 2, 3, 8, 9, 10, 15, 16, and 17). Mice were harvested 24 h after the last treatment. Differential cell counts of monocytes (**b**) and eosinophils (**c**) collected from BAL fluid samples of each experimental group. **d** Total protein concentrations from BAL fluid. Asterisks represent $p < 0.05$. Error bars represent SD

Author Manuscript Author Manuscript Author Manuscript Author Manuscript

Table I.

Experimental Groups

Experimental group	Conditions
Control (C) (n = 4)	No exposure to HDM challenge or drug treatment
HDM challenge only (HDM) (n = 8)	Exposure to HDM challenge, without drug treatment
HDM challenge and Vehicle treatment (HDM+V) (n = 8)	Exposure to HDM challenge; treatment with nebulized vehicle
HDM challenge and low-dose drug treatment (HDM+LD) (n = 8)	Exposure to HDM challenge; treatment with nebulized tofacitinib citrate at a low dose
HDM challenge and high-dose drug treatment (HDM+HD) (n = 8)	Exposure to HDM challenge; treatment with nebulized tofacitinib citrate at a high dose

AAPS PharmSciTech. Author manuscript; available in PMC 2019 October 29.